94. Gordon, J. L., *Biochem. J.*, 1986, **233**, 309–319.
95. Ziganshin, A. U., Hoyle, C. H. V. and Burnstock, G., *Drug Dev. Commun.*, 1994, **32**, 134–146.
96. Manchanda, R., D. Phil. Thesis, University of Oxford, 1989.
97. del Castillo, J. and Katz, B., *Proc. R. Soc. London*, 1957, **B146**, 362–368.
98. Fatt, P. and Katz, B., *J. Physiol.*, 1951, **115**, 320–370.
99. Kuba, K. and Tomita, T., *J. Physiol.*, 1971, **213**, 533–544.
100. Magleby, K. L. and Stevens, C. F., *J. Physiol.*, 1972, **223**, 151–171.
101. Walker, J. A. and Wheeler, R. P., *Biochem. J.*, 1975, **151**, 439–442.
102. Evans, R. J. and Kennedy, C., *Br. J. Pharmacol.*, 1994, **113**, 853–860.
103. Ziganshin, A. U., Hoyle, C. H. V., Ziganshina, L. E. and Burnstock, G., *Br. J. Pharmacol.*, 1994, **113**, 669–674.
104. Holman, M. E. and Suprenant, A., *Br. J. Pharmacol.*, 1980, **71**, 651–661.
105. Cheung, D. W., *J. Physiol.*, 1982, **328**, 449–459.
106. Cheung, D. W., *J. Physiol.*, 1982, **328**, 461–468.
107. Sneddon, P. and Burnstock, G., *Eur. J. Pharmacol.*, 1984, **106**, 149–152.
108. Ishikawa, S., *Br. J. Pharmacol.*, 1985, **86**, 777–787.
109. von Kügelgen , I-v. and Starke, K., *J. Physiol.*, 1985, **367**, 435–455.
110. Muramatsu, I., *Br. J. Pharmacol.*, 1986, **87**, 478–480.
111. Cheung, D. W. and Fujioka, M., *Br. J. Pharmacol.*, 1986, **89**, 3–5.
112. Burnstock, G. and Kennedy, C., *Circ. Res.*, 1986, **58**, 319–330.
113. Matsuoka, T., Komori, S. and Ohashi, H., *Br. J. Pharmacol.*, 1994, **110**, 87–94.
114. Fujii, K., *J. Physiol.*, 1988, **404**, 39–52.
115. Sneddon, P. and McLees, A., *Eur. J. Pharmacol.*, 1992, **214**, 7–12.
116. Ohno, N., Kaoru, M. I., Yamamoto, Y. and Suzuki, H., *Eur. J. Pharmacol.*, 1993, **249**, 121–123.
117. Zagorodnyuk, V. and Maggi, C. A., *Br. J. Pharmacol.*, 1994, **112**, 1077–1082.
118. Benham, C. D., *Nature*, 1992, **359**, 103.
119. Edwards, F. A., Gibb, A. J. and Colquhoun, D., *Nature*, 1992, **359**, 144–147.
120. Evans, R. J., Derkach, V. and Suprenant, A., *Nature*, 1992, **357**, 503–505.
121. Silinsky, E. M. and Gerzanich, V., *J. Physiol.*, 1993, **464**, 197–212.
122. Hirst, G. D. S. and Neild, T. O., *Nature*, 1980, **283**, 767–768.
123. Hirst, G. D. S. and Neild, T. O., *J. Physiol.*, 1981, **313**, 343–350.
124. McGrath, J. C., *Nature*, 1980, **288**, 301–302.
125. Hirst, G. D. S. and Neild, T. O., *Nature*, 1981, **288**, 302.
126. Bevan, J. A., *Trends Pharmacol. Sci.*, 1984, **5**, 53–55.
127. Neild, T. O. and Hirst, G. D. S., *Trends Pharmacol. Sci.*, 1984, **5**, 56–57.
128. Kuffler, S. W. and Yoshikami, D., *J. Physiol.*, 1975, **251**, 465–482.
129. Brock, J. A. C. and Cunnane, T. C., in *Autonomic Neuroeffector Mechanisms* (eds Burnstock, G. and Hoyle, C. H. V.), Harwood Academic Publishers, Switzerland, 1992, pp. 121–213.
130. Kostron, H., Winkler, H., Peer, L. J. and König, P., *Neuroscience*, 1977, **2**, 159–166.
131. Bültmann, R. Driessen, B., Conçalves, J. and Starke, K., *Naunyn. Schmeid. Arch. Pharmacol.*, 1995, **351**, 555–560.
132. Brown, G. L., *Proc. R. Soc. London*, 1964, **162**, 1–19.
133. Burnstock, G., *Neuroscience*, 1976, **1**, 239–248.
134. Morris, J. L. and Gibbins, I. L., in *Autonomic Neuroeffector Mechanisms* (eds Burnstock, G. and Hoyle, C. H. V.), Harwood Academic Publishers, Switzerland, 1992, pp. 121–213.

Received 8 December 1995; accepted 30 January 1996

Covariant differentials lead to the design of a novel self-tuning power system stabilizer

D. P. Sen Gupta and Indraneel Sen

Department of Electrical Engineering, Indian Institute of Science, Bangalore 560 012, India

Application of differential geometry to study the dynamics of electrical machines by Gabriel Kron evoked only theoretical interest among the power system engineers and was considered hardly suitable for any practical use. Extension of Kron's work led to a physical understanding of the processes governing the small oscillation instability in power system. This in turn has made it possible to design a self-tuning Power System Stabilizer to contain the oscillatory instability over an extended range of system and operating conditions. This paper briefly recounts the history of this development and touches upon the essential design features of the stabilizer. It presents some results from simulation studies, laboratory experiments and recently conducted field trials at actual plants – all of which help to establish the efficacy of the proposed stabilizer and corroborate the theoretical findings.

THE application of tensor calculus in analysing the performance of electrical machines was initiated by Gabriel Kron in the thirties[1]. Criticized by physicists for his intrusion into Riemannian geometry, needed for the de-

scription of the electrodynamics of an electrical machine in the complex space–charge–time system, Kron was derided by fellow engineers for making life unnecessarily difficult. Banesh Hoffman[2], the Relativist, came to Kron's rescue and Lynn[3] made Kron's work more comprehensible. The engineers still rejected them as far too abstract and of little use to design anything useful. The use of covariant differentials, seldom used by electrical engineers, has now made it possible to design and test a self-tuning Power System Stabilizer (PSS), a much needed device for suppressing low-frequency oscillations in power systems. This paper describes the essential features of the design and the results of successful testing of this stabilizer at an actual power plant.

A generator delivering power is usually synchronized to a large power system. At steady state, the magnetic fields set up by the armature and the field coils of all generators rotate at the same synchronous speed. Any small perturbation in the system causes individual rotors to oscillate about the synchronous speed. These low-frequency oscillations of about 1 Hz, described as hunting, were first observed in early thirties. The problem was overcome by incorporating damper windings in the generators which dissipated the kinetic energy associated with the rotor oscillations by causing $\Delta i^2 R$ losses in closed circuit coils.

In late sixties, by which time power systems had grown vastly and were considerably more complex, low-frequency oscillations started to reappear. Major instabilities in the system were reported by many power utilities around the world[4]. Nearer home, the first 210 MW generator of the Raichur Thermal power plant could only deliver 160 MW. A marginal increase in its loading caused low-frequency oscillations. The cause of this low-frequency oscillation was traced to the increasing use of fast acting, solid state Automatic Voltage Regulators (AVRs). An AVR tries to maintain the generator output voltage constant by modulating the excitation current in response to the changes in the terminal voltage V_t.

Additional controllers were required to counter this destabilizing effect of the AVR. It was found that a signal derived from changes in the angular velocity ($\Delta\omega$), delivered power (ΔP) and frequency (Δf) during oscillations, could be mixed with the ΔV_t input to stabilize the system. The gains and the phases of these signals however have to be properly adjusted before the stabilizing signal could be fed back into the system. This process, called the tuning of the stabilizer, causes a major problem as the complex gains (K_ω, K_p and K_f) selected for a particular system and operating condition are generally not suitable for other conditions.

In the last decade there has been considerable research on the design of variable gain or adaptive power system stabilizers[5,6]. However, for all practical purposes, these have not been implemented on actual systems because of the complexity of computation in real time and the possibilities of numerical instabilities with catastrophic consequence.

It is in this area of research that some of Kron's original ideas could be successfully applied. Based on Kron's method, by a rigorous analysis it could be shown that negative damping is produced by long transmission lines. The damper windings, however, compensate for this negative damping[7]. The reappearance of the oscillations referred to earlier was therefore intriguing. It was suspected that the AVR–rotor circuit was the source of negative damping because increasing the gain of the AVR for better voltage control greatly enhanced the possibilities of the low-frequency oscillations[8,9].

This indeed is the case. The use of tensor analysis has enabled us to exactly quantify the negative damping produced by the AVR circuit. A PSS can now be designed to generate an equal amount of positive damping to exactly cancel the negative damping in the system at all operating conditions.

Electrical machine – A geometrical view

An electrical machine essentially comprises a set of current carrying coils rotating w.r.t. another set of coils. If all the coils were stationary, the coil voltages could be expressed as,

$$e_\alpha = R_{\alpha\beta} i^\beta + L_{\alpha\beta} \frac{\mathrm{d}i^\beta}{\mathrm{d}t}, \tag{1}$$

where e_α is the covariant voltage vector, i^β the contravariant current vector, $R_{\alpha\beta}$ the resistance matrix and $L_{\alpha\beta}$ the inductance matrix with the self-inductances of the coils as the diagonal and the mutual inductances as off-diagonal elements.

When the coils rotate w.r.t. each other, the voltage equation gets modified to,

$$e_\alpha = R_{\alpha\beta} i^\beta + L_{\alpha\beta} \frac{\delta i^\beta}{\mathrm{d}t}, \tag{2}$$

where $\delta i^\beta/\mathrm{d}t$ represents the covariant derivatives of the current given by,

$$\frac{\delta i^\beta}{\mathrm{d}t} = \frac{\mathrm{d}i^\beta}{\mathrm{d}t} + \{\alpha\ {}^\beta\tau\} i^\beta \frac{\mathrm{d}\theta^\tau}{\mathrm{d}t}. \tag{3}$$

$\{\alpha\ {}^\beta\tau\}$ is the Christoffel symbol of the second kind and in the present case is given by,

$$\{\alpha^\beta\tau\} = \frac{1}{2} L^{\beta\delta}\left[\frac{\partial L_{\tau\beta}}{\partial i^\alpha} + \frac{\partial L_{\beta\alpha}}{\partial \theta^\tau} - \frac{\partial L_{\alpha\tau}}{\partial i^\beta}\right]. \tag{4}$$

The inductances constitute the metric tensors. The dimension of the space depends upon the number of coils carrying independent currents. Interconnected coils give rise to a subspace embedded in the original space. If the saturation effects are neglected, $\partial L/\partial i$ terms become

zero and the inductances are only functions of the rotor position θ. Since the magnetic paths linking the various coils in an electrical machine are irregular, $\partial L/\partial\theta$ terms assume extremely complex forms.

To overcome this difficulty, the stator windings can be transformed into a set of fictitious coils which are stationary w.r.t. the synchronously rotating rotor coils. In one of the most commonly used transformations, called the Park's transformation, the observer is fixed to the rotor and observes all the changes that take place in the system. In steady state, the rotor and the stator fields rotate synchronously and thus appear stationary w.r.t. each other. In Park's frame of reference, the relationship between the coordinates is implicitly expressed in terms of the differentials of the coordinates. In a synchronous machine when the stator currents are transformed to the rotor reference frame, the resulting relationship is in nonintegrable form and the transformation is 'non-holonomic'. An additional geometric object appears in the differential expression which is defined as

$$\Omega^{\tau}_{\alpha\beta} = \frac{1}{2} C^{\mathrm{a}}_{\alpha} C^{\mathrm{b}}_{\beta} \left[\frac{\partial C^{\tau}_{\mathrm{a}}}{\partial X^{\mathrm{b}}} - \frac{\partial C^{\tau}_{\mathrm{b}}}{\partial X^{\mathrm{a}}} \right], \tag{5}$$

and in a non-holonomic reference frame, the Affine connection $\Gamma^{\Pi}_{\alpha\beta}$ is expressed as

$$\Gamma^{\Pi}_{\alpha\beta} = g^{\Pi\delta}[\alpha\beta, \delta] + g^{\Pi\delta} g_{\beta\sigma} \Omega^{\sigma}_{\delta\alpha} + g^{\Pi\delta} g_{\alpha\sigma} \Omega^{\sigma}_{\delta\beta} - \Omega^{\Pi}_{\alpha\beta} \tag{6}$$

where g is the usual metric tensor inductances in the present case.

The voltage equation of all the rotating coils can be therefore written in the most general form as

$$e_{\alpha} = R_{\alpha\beta} i^{\beta} + L_{\alpha\beta} \frac{\mathrm{d}i^{\beta}}{\mathrm{d}t} + \Gamma_{\beta\tau,\alpha}\, i^{\beta} \frac{\mathrm{d}\theta^{\tau}}{\mathrm{d}t}. \tag{7}$$

$L_{\alpha\beta}\, \mathrm{d}i^{\beta}/\mathrm{d}t$ represents the 'transformer' voltage induced due to the rate of change of current and $\Gamma_{\beta\tau,\,\alpha}\, i^{\beta}\mathrm{d}\theta/\mathrm{d}t$ represents the 'speed' voltage generated due to the motion of the coil in the magnetic field.

During rotor oscillations, oscillating currents are induced in all the coils, superimposed on the steady state currents. As stated earlier, these currents cause ohmic losses ($\Delta i^2 R$) in each coil which help in dissipating the kinetic energy associated with the oscillating rotor.

The computation of the losses due to the oscillating currents Δi, in the rotor circuit (the field and the damper windings), using Park's frame of reference gives correct results as there is no relative movement of the coils w.r.t. the Park's axes. Similar computation of losses for the stator circuit, however, always results in wrong estimation of losses.

Park's transformation, so far as the rotor coils are concerned, is holonomic and the Affine connection reduces to the Christoffel symbol. The incremental currents in the rotor coils can therefore be expressed as,

$$\delta i^{\alpha} = \Delta i^{\alpha} + \{\beta\ {}^{\alpha}\tau\}\ i^{\beta} \Delta\theta^{\tau}. \tag{8}$$

Since viewed from Park's frame of reference, the inductances appear to be constant, the metric tensor is constant and the Christoffel symbol in equation (3) is zero. This implies $\delta i = \Delta i$, that is, the changes in currents that appear to take place in the rotor coils from Park's axes are also the true or absolute changes.

For stator coils, the Park's transformations are non-holonomic and

$$\delta i^{\alpha} = \Delta i^{\alpha} + \Gamma^{\alpha}_{\beta\tau} i^{\beta} \Delta\theta^{\tau}. \tag{9}$$

Although the Chirstoffel symbol contained in the Affine connection $\Gamma^{\alpha}_{\beta\tau}$ is zero, the Ω terms (eqs (5), (6)) are non-zero. As a result, $\delta i^{\alpha} \neq \Delta i^{\alpha}$ and the apparent changes do not represent the actual incremental changes taking place in the stator coils.

This explains why efforts to relate damping to ohmic losses by standard methods did not succeed. The damping has to be computed using δi, the actual changes in currents and not Δi, which represent the apparent changes.

A geometrical interpretation of these changes (see Appendix for details) confirms Kron's conclusion that in case of a synchronous machine, $\Gamma^{\alpha}_{\beta\tau}$ reduces to a simple rotation tensor ρ given by

$$\rho = \begin{array}{|c|c|} \hline & 1 \\ \hline -1 & \\ \hline \end{array}. \tag{10}$$

The realization that absolute changes in the stator currents and not the apparent changes need to be considered when computing losses has enabled us to exactly quantify the losses in various coils and prove that during hunting the sum of the losses add up to the total losses in the system (see Table 1).

Table 1. Components of total damping at a typical operating condition

	Oscillating currents			
	Apparent change	Absolute change	Copper loss	
Windings	Δi *pu*	δi *pu*	$\Delta i^2 R$ *pu*	$\delta i^2 R$ *pu*
Field	$-0.0045 - j0.0985$	$-0.0045 - j0.0985$	0.04867	0.04867
Armature				
F-axis*	$0.1526 + j0.300$	$0.0660 + j0.475$	−0.03970	−0.08080
B-axis	$0.1327 - j0.169$	$0.0460 - j0.344$	0.01550	0.04050
		Total	0.02447	0.00837

T_{D}, damping torque coefficient $= \dfrac{\text{copper loss}}{\text{hunting freq. } h}$.

T_{D}, based on apparent change $(\Delta i) = (0.02447/0.0216) = 1.138$

T_{D}, based on apparent change $(\delta i) = (0.00837/0.0216) = 0.3875$

Actual measured $T_{\mathrm{D}} = 0.3875$

*The resistance in armature *F*-axis $= R_a/(h-1)$ and for $h < 1$, copper loss is negative.

Once it was established that the total losses in the system could indeed be equated to $\Sigma\delta i^2 R$, it was possible to establish that the damping produced in the regulator circuit T_{DR}, is exactly proportional to the incremental power input into the AVR circuit or,

$$T_{DR} = K_A\, Re\, (\Delta V_t\, \Delta i_f^*)/h^2$$
$$= K_A\, (\Delta V_t\, \Delta i_f \cos \Phi)/h^2, \qquad (11)$$

where K_A is the AVR gain, ΔV_t is the change in the terminal voltage and Δi_f is the change in field current. This expression for T_{DR}, unlike some other expressions[9], is direct and has considerable physical significance. It has been seen that for most operating conditions the angle Φ or the angle between the injected voltage to the AVR and the resulting change in the current Δi_f is larger than 90°. This is only possible when the field circuit appears to have a negative resistance. Since positive $\Delta i^2 R$ provides positive damping, $\Delta i^2(-R)$ provides negative damping and helps in building up the oscillations.

The AVR damping torque is usually negative when the load and the AVR gains are large and the feedback time constant is negligibly low (the characteristic features of a modern solid state excitation system). Having established the relation given in equation (11) the reasons for T_{DR} becoming negative can now be investigated.

The change in terminal voltage is contributed by various changes in the system and can be expressed in terms of changes in field excitation, rotor speed and the load angle as follows,

$$\Delta V_t = K_f \Delta i_f + K_\omega \Delta\omega + K_\delta \Delta\delta, \qquad (12)$$

or by an equivalent expression,

$$\Delta V_t = K_f \Delta i_f + K_\omega \Delta\omega + K_p \Delta P. \qquad (13)$$

Multiplying both sides by Δi_f^*, the complex conjugate of Δi_f, the expression modifies to,

$$\Delta V_t \Delta i_f^* = K_f \Delta i_f \Delta i_f^* + K_\omega \Delta\omega \Delta i_f^* + K_p \Delta P \Delta i_f^*. \qquad (14)$$

It can be shown that[10] K_f is almost always positive in single machine power systems, $\Delta i_f \Delta i_f^*$ is always positive and if negative damping is being produced in the regulator circuit, it must originate from the $K_\omega \Delta\omega \Delta i_f^* + K_p \Delta P \Delta i_f^*$ terms. Needless to point out again that viewed from the rotor (or the field circuit) $\delta i_f = \Delta i_f$ and ΔP and $\Delta\omega$ are the actual measured changes in power and angular frequency.

It is now obvious that if an auxiliary signal of the form

$$V_{pss} = K_\omega\, \Delta\omega + K_p \Delta P \qquad (15)$$

with proper choice of K_ω and K_p is mixed with the ΔV_t signal, the negative damping produced in the system can be exactly cancelled.

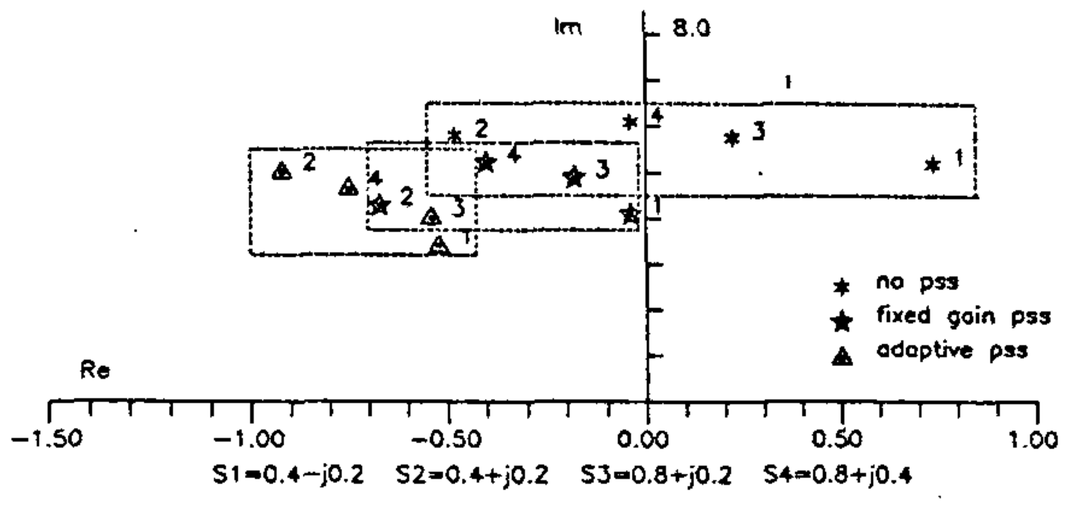

Figure 1. Rotor mode eigenvalues with and without PSS at four operating conditions.

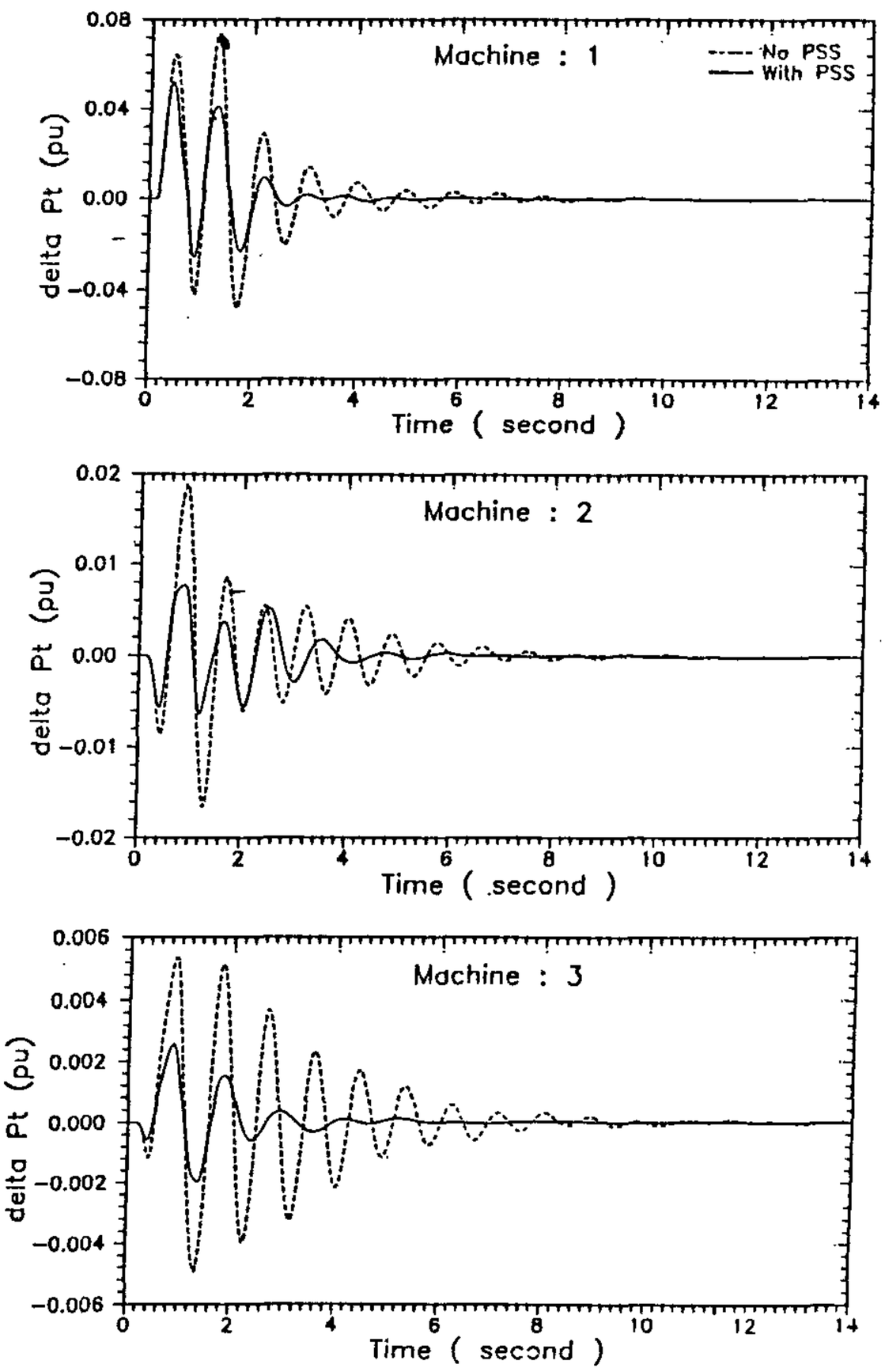

Figure 2. System response with and without the proposed adaptive stabilizer in a 3-machine configuration.

As the negative damping produced in the system which changes with the system and operating conditions has been quantified, exact expressions relating the gains K_ω and K_p to system and operating conditions to neutralize the negative damping can now be obtained. In case

of more complex power systems, where K_f could be negative, expressions relating K_ω and K_p to system and operating conditions can still be found to cancel the negative damping produced by the AVR[10]. The tuning of stabilizer is thus no longer based on trial and error and the stabilizer's performance can therefore be maintained over an extended range of system and operating conditions.

Performance analysis on computer simulated models

Extensive computations have established that the PSS designed on the concept of cancelling negative damping not only improves the dynamic stability of the system significantly but the gains K_ω and K_p adapt themselves to changing operating and system conditions, keeping the generator well within the stability boundary.

Figure 1 shows the rotor mode eigenvalues of a system for three cases: (a) when no PSS is used, (b) when a conventional fixed gain PSS is used and (c) when the proposed self-tuning stabilizer is used at four different operating conditions. So far as the fixed gain stabilizer is concerned, it has to be tuned on site which calls for high level of expertise and even then the performance degrades as the system and operating conditions change. On the other hand, the adaptive gains need no pre-setting and are self-tuning for optimum performance. This is evident from the eigenvalue plots which show better damping as compared to the fixed gain stabilizer at all operating conditions.

Typical transient responses of three generators in a mutimachine system with and without the proposed stabilizer are shown in Figure 2. In this multimachine system, multiple frequencies of oscillations are present. Considerable improvement in system performance at all machines is clearly evident. The adaptive PSS is thus capable of damping out the multimodal oscillations.

Laboratory experiments and field tests

The performance of the proposed power system stabilizer has been evaluated on a scaled model of a power system in the laboratory. The system comprising a microalternator representing 500 MW generator, a steam turbine simulator and 1200 km of 400 kV microtransmission line is interfaced with a computer to generate the stabilizing signal by computing the gains K_ω and K_p based on real time measurement. The adaptive stabilizer was quite effective in damping the low-frequency oscillations over a wide range of operating conditions. Some of the test results are shown in Figure 3. The system responses are highly oscillatory in all the three cases but

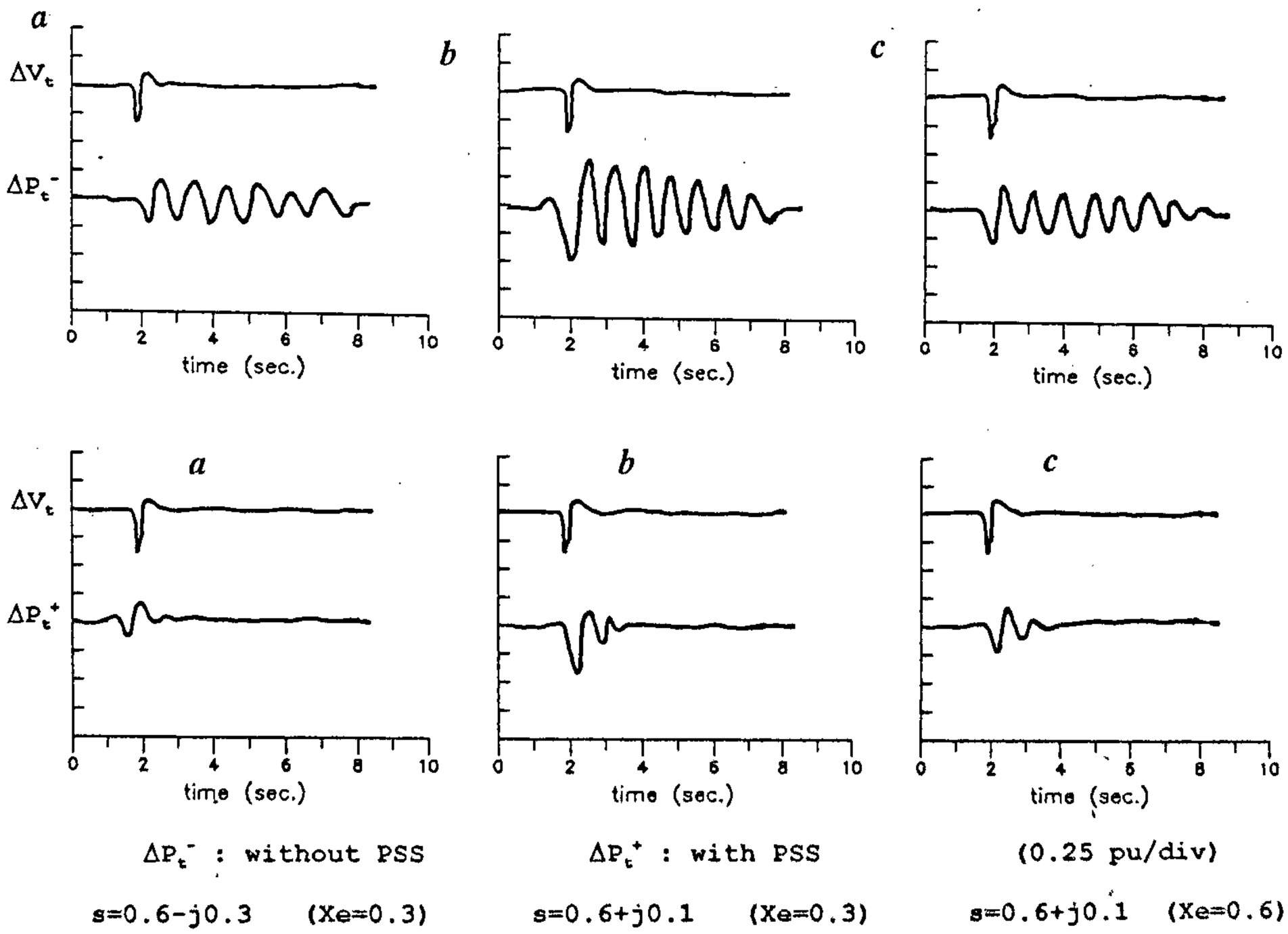

Figure 3. System response with and without the proposed adaptive stabilizer in a laboratory model of power system.

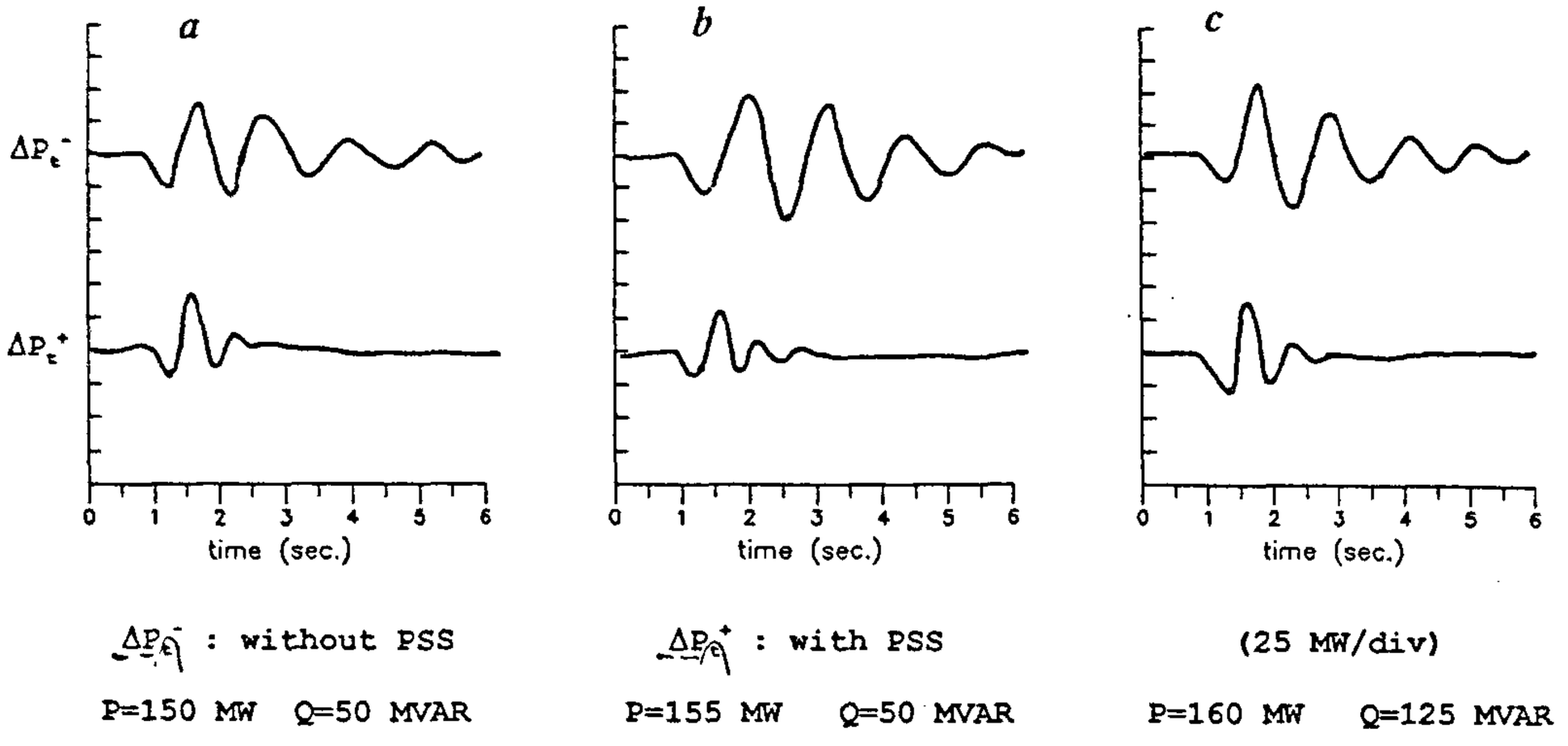

Figure 4. System response with and without the proposed adaptive stabilizer on the 210 MW thermal unit at Mettur Power Plant.

are very well damped when the proposed stabilizer is used. The system depicted in Figure 3 *c* which is very close to losing synchronism is stabilized within two cycles when the stabilizer is in use.

Following the successful testing in the laboratory, a prototype model of the stabilizer was recently built for testing at actual power plants, one at Mettur, on a 210 MW thermal unit and the other at Varahi, on a 115 MW hydel unit. Despite the limited variations in the operating and system conditions, permissible in a major generating plant in operation, the superiority in performance of the adaptive stabilizer *vis-a-vis* the currently installed fixed gain stabilizer could easily be established. The performance of the stabilizer at three operating conditions is shown in Figure 4.

Conclusion

Although the use of differential geometry for analysing an electrical machine has not found much favour with the engineers, it has presented a totally new approach to the design of a simple controller that can stabilize an oscillating power system. The use of covariant differentials has made it possible to exactly quantify the positive and negative damping contributions of the various windings of the generator. The negative damping contributed by the AVR can therefore be estimated and a stabilizer could be designed to cancel this negative damping. Further studies have shown that this stabilizer can also selectively damp out multimodal oscillations experienced by synchronous generators in large systems. This will enable generators which are prone to oscillations, to deliver power up to their rated capacity even when all other system conditions may vary over a wide range.

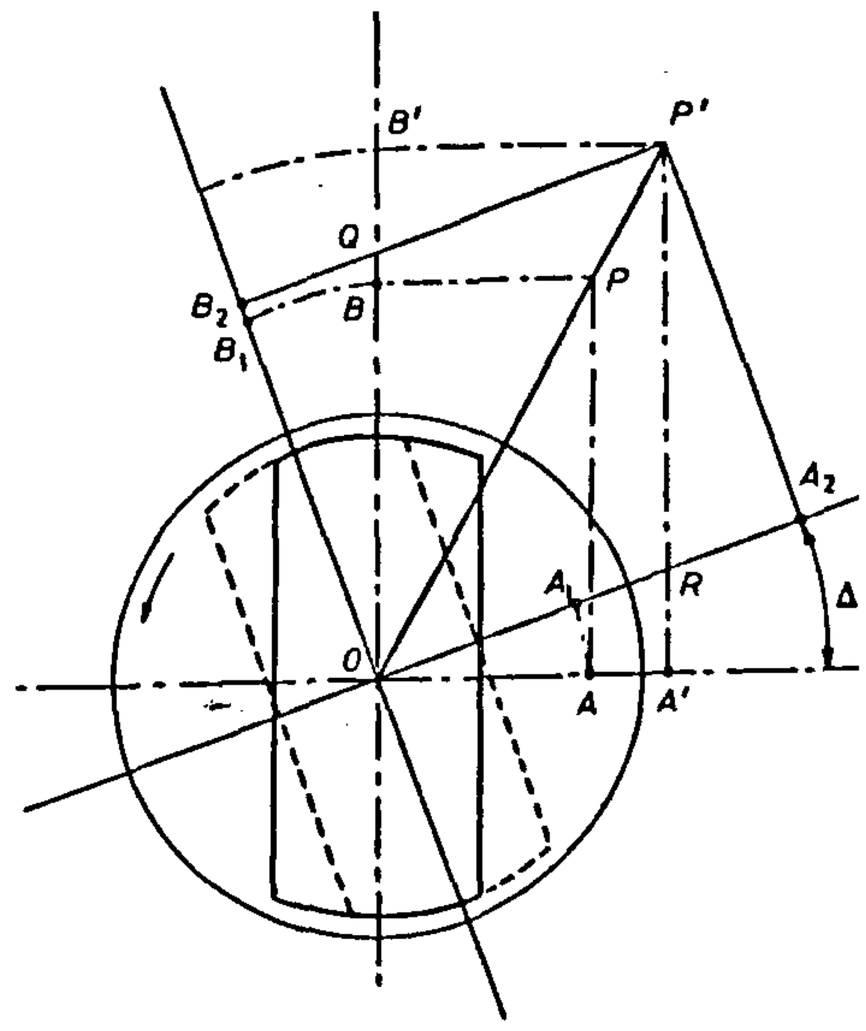

Figure 5. Changes in armature current and mmf as seen from and Kron's axes. (The apparent and absolute changes).

Appendix

Figure 5 is a schematic representation of a synchr machine. The rotor is represented as an electroma In Park's frame of reference, the observer is tied t synchronously rotating rotor and during rotor os tions, the observer oscillates along with the roto observer on Kron's axes also rotates at synchr speed but as the axes are decoupled from the roto observer does not oscillate with the rotor. Let OP r

sent a synchronously rotating mmf vector corresponding to the stator currents. The components of this vector, at a particular instant are OB along the axis of the pole (d-axis) and OA along the quadrature or the q-axis. During oscillation, let the vector OP still rotating synchronously, be increased by PP′ and let the rotor occupy the dotted position displaced from the original position by an angle $\Delta\theta$. The component of OP′ along the d-axis is now OB_2 and OA_2 along the q-axis. According to the observer, the change in vector OP is B_1B_2 along its d-axis and A_1A_2 along the q-axis and the total change is therefore, $(B_1B_2^2 + A_1A_2^2)^{1/2}$, which is incorrect. If the observer did not move with the rotor (Kron's axis) and rotated synchronously, he would have measured BB′ and AA′ as the respective changes and would estimate the total change as $(BB'^2 + AA'^2)^{1/2}$ which is the actual change. It may be seen that neglecting the second order effects,

$$AA' = A_1A_2 - PA \cdot \Delta\theta,$$

or $$\delta i_q = \Delta i_q - i_d \cdot \Delta\theta$$

and $$\delta i_d = \Delta i_d - i_q \cdot \Delta\theta,$$

or $$\begin{bmatrix} \delta i_d \\ \delta i_q \end{bmatrix} = \begin{bmatrix} \Delta i_d \\ \Delta i_d \end{bmatrix} + \begin{bmatrix} 0 & 1 \\ -1 & 0 \end{bmatrix} \begin{bmatrix} i_d \\ i_q \end{bmatrix} \cdot \Delta\theta$$

or $$\underline{\delta i} = \underline{\Delta i} + \underline{\rho i}\Delta\theta$$

where ρ is the rotation tensor.

1. Kron, G., *J. Math. Phys*, 1934, **13**, 103–194.
2. Hoffmann, B., *Q. Appl. Math.*, 1944, **II**, 218–281.
3. Lynn, J. W., *Tensors in Electrical Engineering*, Edward Arnold Publishers, London, 1963.
4. Hanson, O. W., Goodwin, C. J. and Dandeno, P. L., *IEEE Trans. Power Appar. Syst.*, 1968, **87**, 276–282.
5. Kannaiah, J., Malik, O. P. and Hope, G. S., *IEEE Trans. Power Appar. Syst.*, 1984, **103**, 897–910.
6. Wu, Q. H. and Hogg, B. W., *Proc. IEE*, 1990, **137**, 146–158.
7. Sen Gupta, D. P., Balasubramaian, N. V. and Lynn, J. W., *Proc. IEE*, 1967, **114**, 1451–1457.
8. Jacovides, L. J. and Adkins, B., *Proc. IEE*, 1966, **113**, 1021.
9. De Mello, F. and Concordia, C., *IEEE Trans. Power Appar. Syst.*, 1969, **88**, 316–329.
10. Ghosh, F., M Sc Thesis, Indian Institute of Science, Bangalore, 1991.

Received 15 December 1995; accepted 8 January 1996

Probable influence of Tehri reservoir load on earthquakes of the Garhwal Himalaya

R. Chander and Kalpna

Department of Earth Sciences, University of Roorkee, Roorkee 247 667, India

Our mathematical simulation suggests that the Tehri reservoir load may produce relatively small changes in the stabilities of nearby seismogenic faults and lead to comparable small advancements or postponements in the times of occurrence of earthquakes of the Garhwal Himalaya.

THE nature and extent of the environmental impact of the proposed Tehri reservoir (Figure 1) is a matter of considerable concern. A major apprehension is that the reservoir may trigger earthquakes. We examine here the possibility of an adverse influence of the reservoir on local seismicity through numerical simulations.

We may clarify at the outset that a man-made reservoir may influence local seismicity through firstly, load-induced stresses and secondly, pore pressure effects. The present study is an examination of only the load effects of Tehri reservoir because virtually nothing is known about the subsurface hydraulic regime in the region of interest. A partial study of this type appears justified because we should assess at least those effects of Tehri reservoir that we can with some degree of confidence with the resources at our command. Further comments which tend to mitigate partially the consequences of ignoring the pore pressure effects are given below.

The basis for the simulation

We assume that the problem may be examined through the following two-step procedure. Firstly, we may use the available seismological information to identify the hypocentral regions as well as the causative faults of future earthquakes around the Tehri reservoir region. It is implicit here that the hypocentres will lie in the causative faults. Secondly, we may assess the time (t) dependent influence of the reservoir load at a future hy-